NJC

Accepted Manuscript

This is an *Accepted Manuscript*, which has been through the Royal Society of Chemistry peer review process and has been accepted for publication.

Accepted Manuscripts are published online shortly after acceptance, before technical editing, formatting and proof reading. Using this free service, authors can make their results available to the community, in citable form, before we publish the edited article. We will replace this *Accepted Manuscript* with the edited and formatted *Advance Article* as soon as it is available.

You can find more information about *Accepted Manuscripts* in the Information for Authors.

Please note that technical editing may introduce minor changes to the text and/or graphics, which may alter content. The journal's standard Terms & Conditions and the Ethical guidelines still apply. In no event shall the Royal Society of Chemistry be held responsible for any errors or omissions in this *Accepted Manuscript* or any consequences arising from the use of any information it contains.

ROYAL SOCIETY OF CHEMISTRY

www.rsc.org/njc

Journal Name

ARTICLE

3(2H)-Furanone as a promising scaffold for the synthesis of novel fluorescent organic dyes: An experimental and theoretical investigation

Received 00th January 20xx,
Accepted 00th January 20xx

DOI: 10.1039/x0xx00000x

www.rsc.org/

Beena Varghese,[a] Saleh N. Al-Busafi[a], FakhrEldin O. Suliman[*] and Salma M. Z. Al-Kindy[a]

3(2H)-Furanones are a type of five-membered heterocyclic compounds of synthetic and biological importance. For exploring the utilities of this "sweet" aroma component for bio-analytical purposes we have prepared and characterized two novel fluorophores (2Z)-2-(5-fluoro-2-ntro benzylidene)-5-phenyl-3(2H)-furanone (FNPF) and (2Z)-2-(4-carboxy benzylidene)-5-phenyl-3-(2H)-furanone (CBPF) on 3-furanone skeleton. In order to expand their application potential, photophysical properties have been investigated using absorption and emission spectroscopy, in combination with quantum chemical calculations. As expected, both compounds showed efficient solvatochromic properties and the excited state dipole moments are larger than those of the ground state. Solvent dependent spectral data using TD-DFT calculations on the optimized ground and excited state structures of both compounds were found to correlate well with the experimental findings.

1. Introduction

Fluorescent probes have been used extensively for investigation of biological systems such as in sensing the polarity of micro-environments of proteins, lipids and DNA and for labelling [1]. 3(2H)-Furanones are a type of five-membered heterocyclic compounds of synthetic and biological importance. The importance of this type of compounds stem from the facile opening of the lactone ring to give acyclic products, which undergo ring closure to give other synthetically and biologically useful heterocyclic compounds [2]. Apart from its many uses in synthetic chemistry, these synthetic building blocks are rather expensive. Therefore, the synthesis, and properties of these compounds have attracted much attention from the synthetic organic chemists and biologists.

Furthermore, the 3(2H)-furanone ring system have attracted much more attention as valuable targets than other furan derivatives due to their presence as a subunit in many natural products isolated from a variety of sources like sponges, algae, animals, plants and insects [3]. This core unit is the key structure to induce a wide range of biological activities like antimicrobial [4], antifungal [5], anti-inflammatory [6], anticancer [7] and anti-viral HIV-1 [8]. Natural antitumor agents for example, jatrophone [9], eremantholides [10], geiparvarin [11], chinolone and ciliarin [12] all belong to the group of 3(2H)-furanones.

Synthetic approaches to the 3(2H)-furanone ring system which vary in their degree of flexibility have appeared in the literature [13-21]. Although a number of syntheses of 3(2H)-furanones were known there were in many cases limited to specific substitution patterns. The development of alternative strategies for the preparation of these heterocyclic compounds is therefore of considerable importance and continues to be a challenge. In addition, the biological and pharmacological activity of 3(2H) - furanones have been widely studied; their fluorescent properties were seldom investigated. As a synthetic strategy we reported an efficient three-step synthesis of 5-phenyl furan 3-(2H)-one from benzaldoxime through isoxazole chemistry and its conversion to corresponding fluorophore by simple aldol reaction. These compounds have not been reported previously. Keeping in mind its possible future use for the determination of $-NH_2$ and –OH group by HPLC, we have also studied the environment sensitivity of both compounds in ground and excited state. The observed fluorescence characteristics indicate a conjugation of π – electrons throughout the system via–C=C linkage from the furanone unit to the other end in both compounds. Moreover, the flatter structure of both compounds probably further favours the charge transfer due to higher conjugation between the electron donor and acceptor units. All the preliminary results that we obtained from this study prove that 3-furanone could be an interesting template for the design of novel organic fluorescent dyes which are potentially applicable for bio-analytical purposes.

[a] Department of Chemistry, College of Science, Sultan Qaboos University, Box 36, Al-khod 123, Sultanate of Oman. E-mail: fsuliman@squ.edu.om.; alkindy@squ.edu.om; Phone +968-24141480; Fax: +968-24141469.

† Electronic Supplementary Information (ESI) available:

2. Experimental

2.1 General

All reagents and solvents used in this study were obtained from Sigma-Aldrich Chemical Company and were used without further purification.

Melting points were determined using GallenKamp-MPA350 melting point apparatus. The purity of the synthesised compounds was checked by TLC and analyses were carried out on 0.25 mm thick precoated silica plates (Merk Fertigplatten kieselgel 60F254). Column chromatography was performed using Merk silica gel 60 (40-63 µm). IR spectra were determined on a Perkin-Elmer FTIR-881 spectrometer (Perkin Elmer, USA) using KBr pellets. 1HNMR spectra were recorded using 400 MHz Bruker spectrometer (Bruker Corp.,UK) and in particular, the proton chemical shifts were assigned on the basis of (1H–1H) COSY (Correlated Spectroscopy). 13CNMR spectra were recorded at 100.4 MHz Bruker spectrometer (Bruker Corp., UK) and the multiplicities of 13CNMR resonances were determined by DEPT (90,135) experiments. Chemical shifts (δc) are quoted in parts per million (ppm) to the nearest 0.1 and 0.01 and are referenced to the solvent peak (CDCl3). Mass spectra were obtained using Quattro Ultima Pt tandem quadruple mass spectrometer (Waters Corp. MA, USA) instrument. High resolution mass spectra were obtained using Waters LCT Premier XE Mass Spectrometer instrument determined at the University of Sheffield, UK).

A Shimadzu (model multispec-1501) UV-Vis spectrophotometer (Shimadzu, Japan) and a Perkin Elmer (model LS 55) Luminescence spectrometer (Perkin Elmer, USA) were used to collect absorption and fluorescence spectra, respectively. All measurements were done repeatedly, and reproducible results were obtained. Relative fluorescence quantum yield (φ_f) were determined using quinine sulphate as the reference standard (φ_f =0.55 in 0.1 M H_2SO_4) [22]. Lifetime measurements were performed using a Time Master Fluorescence lifetime spectrometer obtained from Photon Technology International. Excitation was at 380 nm using light emitting diodes. For both compounds, a cut-off filter (400nm, Photon Technology International) was used. The system response time as measured from the scattered light was estimated to be approximately 1.5 ns. The observed decays were fitted to multi-exponential functions convoluted with the instrument response function (IRF). The fit was judged by the value of the reduced chi squared (χ2) values which were close to unity (0.98–1.2).

Cyclic voltammograms of synthesized compounds were recorded by using CV-50 W (BAS, USA)-Voltammetric Analyzer at the scanning rate of 50 mV/sec, over a potential range of -1.5 V to 1.2 V. The electrochemical cell consists of glass carbon electrode as working electrode, Pt wire as a counter electrode and Ag/AgCl as the reference electrode. The stock solution of synthesized compounds was prepared in dimethyl sulfoxide (DMSO) and lithium perchlorate ($LiClO_4$) (0.1M) was used as supporting electrolyte.

2.2 Computational details

The molecular structures of compounds involved in the study were constructed using Chem3D Ultra 10.0. The ground state geometries molecular structures (S_0) of FNPF and CBPF were optimized by the density functional theory (DFT) method using the B3LYP (Becke-three parameter hybrid exchange functional [23] combined with the Lee–Yang–Parr correlation function [24]) employing the 6-31+G (d, p) basis set. The first excited state geometry (S_1) of molecular structure was optimized by the single configuration interaction (CIS) [25], using the same basis set. Estimates of the electronic transition energies, which include some account of the electron correlation, were obtained using the time-dependent density functional theory (TD-DFT) together with the hybrid B3LYP level of theory and using the 6-31+G(d, p) basis set. Absorption spectra were obtained by using the ground state optimized geometry whereas emission energies were obtained considering the CIS optimized structures of the excited state. No symmetry restrictions were imposed to the initial structures; however furanone compounds converged to the planar structures. For the planar structures, no imaginary frequencies were obtained, indicating that they correspond to true minima. Solvent effects (in water & cyclohexane) were also taken into account by using the polarised continuum model (PCM) [26]. All the above calculations were performed using Gaussian 09 programme and GaussView 05 was used for visualisation of structures.

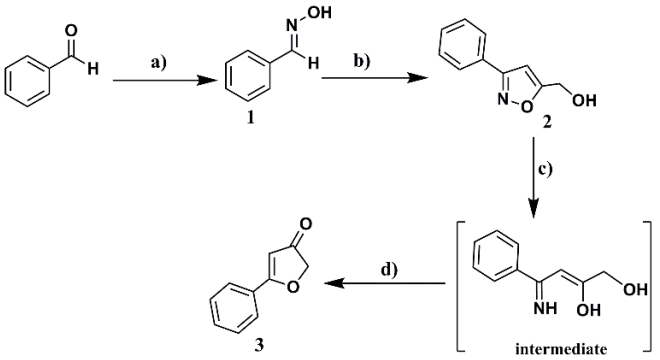

Scheme 1. Reaction conditions: a) $NH_2OH.HCl$, NaOH, stirring; b) $N(CH_2CH_3)_3$, propargyl alcohol , NaOCl, stirring in an ice bath; c) H2, Pd / C; d) H^+, $NaHCO_3$.

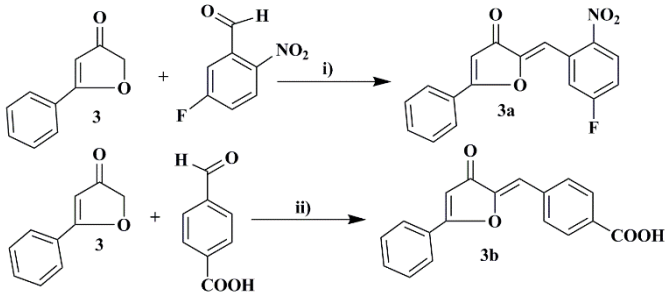

Scheme 2. Reaction conditions: i) K_2CO_3, THF, H_2O, refluxing; ii) KOH, EtOH, H_2O, refluxing.

2.3 Synthesis

The designed target compounds of 3(2H)-furanones (3, 3a, 3b) were synthesized from commercially available starting materials which are illustrated in schemes 1 and 2.

2.3.1 (E, Z) benzaldehyde oxime (1)

To a stirring mixture of sodium hydroxide (8.4 g, 0.21 mol) in 60 ml of distilled water, on regular intervals were added benzaldehyde (12.7 g, 0.12 mol) and hydroxylamine hydrochloride (11 g, 0.144 mol) simultaneously. When the addition was completed, the reaction mixture was neutralized by adding acetic acid drop wise and washed successively with diethyl ether. The ethereal layer was dried over magnesium sulphate, filtered and concentrated under vacuum. Further distillation furnished pure oxime (12.12 g, 83%) as colourless oil. b.p. 136^{0}C at 50 mm of Hg; FTIR (KBr): υ 1602, 3369, 1542, 3650 cm^{-1}; ^{1}H NMR (400 MHz, $CDCl_3$): δ (ppm) 8.18 (s, 1H), 7.57 (m, 2H), 7.42 (m, 3H); ^{13}C NMR (100.4 MHz, $CDCl_3$): δ (ppm) 127.5 (2×CH), 129.2 (2×CH), 131.4 (CH), 133.9 (CH), 151.1 (CH). ESI-MS $[M+H]^+$ calcd. for C_7H_6NO: 121.76, found: 121.14.

2.3.2. 3-phenyl-5-(isoxasolyl) methanol (2)

Propargyl alcohol (4.4 g, 0.079 mol), triethylamine (0.70 g, 0.061 mol) and sodium hypochlorite (300 ml)) were mixed in 175 ml of chloroform. Benzaldoxime (7.4 g, 0. 061 mol) was added dropwise to the cooled reaction mixture. The reaction mixture was further stirred in the ice bath for 45 min. The heterogeneous mixture was separated, and the aqueous layer was extracted with chloroform (3×15 ml). The organic layer was dried, filtered, and concentrated under vacuum. The resulting yellow oil was purified by column chromatography on silica gel using EtOAc / hexane for elution to give compound **2** (7.21g, 68%) as white solid; m.p. 47.3 – 48.2^{0}C; FTIR (KBr): υ 3208, 1609, 1580, 1289 cm^{-1}; ^{1}H NMR(400 MHz,$CDCl_3$): δ (ppm) 7.62-7.65 (m, 2H), 7.30-7.37(m, 3H), 4.66 (S,2H), 6.43 (S,1H); ^{13}C NMR (100.4 MHz, $CDCl_3$) : δ (ppm) 56.7 (CH_2), 100.4 (–C), 127.2 (2×CH), 129.0 (–C), 129.3 (2×CH), 130.5 (CH), 162.9 (–C), 172.7 (–C). ESI-MS $[M+H]^+$ calcd. for $C_{10}H_{10}NO_2$: 177.2, found: 177.1.

2.3.3. 5-phenyl-3(2H)-furanone (3)

A mixture of 3-phenyl-5-(isoxasolyl) methanol (2) (7.06 g, 0.0403 mol) and Pd / C 10% (3.00 g) in methanol (50 ml) was hydrogenated for 6 h. The reaction mixture was filtered and washed with methanol, and the solvent was removed under vacuum to yield a pale red solid. The red solid was dissolved in HCl (1M), and the mixture was stirred for 4 h and then neutralized with saturated $NaHCO_3$. The product was extracted with diethyl ether (3×10 ml) dried, filtered, and concentrated to give red-purple solid. The resulting red-purple solid was purified by column chromatography on silica gel using EtOAc / hexane for elution to give compound **3** (4g, 62%). m.p. 83.4 – 84.5^{0}C; FTIR (KBr): υ 1688.76, 1609.86, 3160, 1281cm^{-1}; ^{1}H NMR(400 MHz,$CDCl_3$): δ (ppm) 7.8–7.9 (m, 2H), 7.4–7.6 (m, 3H), 4.69 (s, 2H), 6.16 (S,1H); ^{13}C NMR (100.4 MHz, $CDCl_3$) :δ (ppm) 75.8 (–CH_2), 101.9 (=CH), 127.4 (2×CH), 130.3 (2×CH), 133.1 (CH), 187.3 (CH), 202.6 (–C=O). ESI-MS $[M+H]^+$ calcd. for $C_{10}H_7O_2$: 160.17, found: 160.15.

2.3.4. (2Z)-2-(5-fluoro-2-nitrobenzylidene)-5-phenyl-3(2H)-furanone (3a)

A mixture of potassium carbonate (1.7 g in 8 ml water), 5 phenyl-3(2H)-furanone (3) (1.0 g, 6.24 mmol), 5-fluro-2-nitrobenzaldehyde (1.1 g, 6.24 mmol) in tetrahydrofuran (8 ml) was kept under reflux overnight. After the complete consumption of starting materials, the heterogeneous mixture was separated, and the aqueous layer was extracted with dichloromethane (4×30 ml). The organic layer was dried, filtered, and concentrated under vacuum. The solid collected was purified by column chromatography on silica gel using EtOAc / hexane for elution to give compound **3a** (1.5 g, 77.4%) as pale yellow solid. m.p.129 –130.6^{0}C; FTIR (KBr): υ 3092.58, 1605.26, 1660.99, 1283.82, 888.5, 1348.91, 1283.82, 539.16 cm^{-1}. ^{1}H NMR (400 MHz,$CDCl_3$) : δ (ppm) 8.15 (dd, J_1= 5.2 Hz, J_2= 9.2Hz, 1H), 7.87 (m, 2H), 7.54-7.65 (m, 4H), 7.23-7.27 (m, 2H), 6.35 (S, 1H);^{13}C NMR (100.4 MHz, $CDCl_3$): δ (ppm) 102.7 (CH), 105.3 (–CH), 116.9 (CH), 119.2 (–CH), 127.07(2×CH), 128.1(–CH), 129.02 (2×CH), 129.71 (–CH), 132.1 (–C), 133.4 (–C), 145.4(–C), 148.1(–C), 163.1(–C), 178.2(–C), 186.6 (–C=O). HRMS (ESI-TOF) m/z: $[M+H]^+$ calcd. for $C_{17}H_9FNO_4$: 312.0672, found 312.0684.

2.3.5. (2Z)-2-(4-carboxybenzylidene)-5-phenyl-3(2H)-furan one (3b)

A mixture of 5-phenyl-3(2H)-furanone (3) (3 g,18.85 mmol), 4-formylbenzoic acid (2.83 g) in 38.3 ml ethanol and aqueous potassium hydroxide (1.3 g in 8 ml distilled water) was refluxed for 2 hours. After stirring at room temperature for another 24 hours, it was acidified by dil. H_2SO_4 drop wise to give orange yellowish precipitate. The solid collected was purified by column chromatography on silica gel using chloroform / methanol / a little amount of water for elution to give compound **3b** (4.5 g, 74%) as yellow solid. m. p.141.6 –142^0 C; FTIR (KBr): υ 1632.83, 1750, 1591.29, 3416.28cm^{-1}; ^{1}H NMR (400 MHz,$CDCl_3$): δ (ppm) 6.81 (S ,1H), 6.87 (S ,1H), 7.67(m, 3H), 8.07(m, 6H) ;^{13}C NMR (100.4 MHz, $CDCl_3$): δ (ppm) 102.8 (=CH), 110.2 (=CH), 127.1 (–C), 127.2 (2×CH), 129.3 (2×CH), 129.9 (2×CH), 131.4 (2×CH), 131.5 (–C), 133.2 (–CH), 135.9 (–C), 146.8 (–C), 166.8 (–C), 177.1 (C=O), 186.4 (C=O). HRMS (ESI-TOF) m/z: $[M+H]^+$ calcd. for $C_{18}H_{11}O_4$: 293.0814, found 293.0827.

3. Results and discussion

3.1. Synthesis

The synthetic strategy employed involves an efficient preparation of the key intermediate 5-phenyl-3(2H)-furanone (**3**) from benzaldehyde in 3-steps. Benzaldoxime (**1**) was prepared in 83% yield from benzaldehyde following standard procedure. 1, 3-dipolar cycloaddition reaction between benzaldoxime (**1**) and propargyl alcohol in the presence of sodium hypochlorite provided 3-phenyl-5-(isoxasolyl) methanol (**2**) in 64% yield. Catalytic hydrogenation of compound 2 in the presence of 10% palladium on charcoal in MeOH occurred smoothly, giving a purple-red solid, which was subsequently subjected to acidic hydrolysis with hydrochloric acid (1M, pH<1) followed by treatment with saturated sodium bicarbonate solution to afford 5-phenyl-3(2H)-furanone (**3**) in 62% yield.

The target compounds **3a** (FNPF) and **3b** (CBPF) were obtained by simple aldol reaction between compound **3** with 5-fluro-2-nitrobenzaldehyde and 4-formylbenzoic acid respectively. Both compounds were isolated and purified by column chromatography on silica gel with high purity. The structures of products 1-3b were characterized by spectroscopic methods (^{1}H NMR, ^{13}C NMR, IR, ESI-MS and HRMS).

3.2. Effect of solvent on the absorption and emission spectra

The absorption spectra of FNPF and CBPF in selected solvents are presented in Fig. 1 and spectroscopic data were collected in Table 1. The values of the absorption coefficient of the studied compounds are ranging from 1.20–5.80×10^4 M^{-1}cm^{-1} for FNPF and 1.28–6.20×10^{4}M^{-1}cm^{-1} for CBPF in different solvents. The absorption band positions broadly lie between 325-344 nm and 295-316 nm for CBPF and FNPF respectively and these wavelength bands were attributed to π-π* transitions originating from 3-furanone moiety. The spectra show that the absorption peak shifted towards red when the solvent is changed from cyclohexane to water for both compounds.

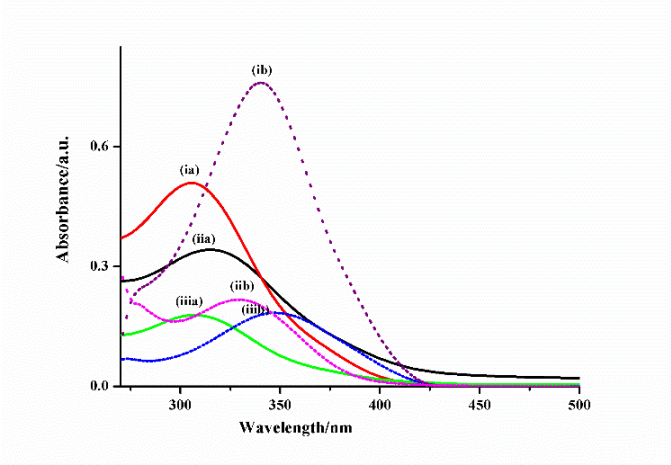

Fig.1.The absorption spectra of FNPF in (ia) THF (iia) water (iiia) cyclohexane and CBPF in (ib) methanol (iib) chloroform (iiib) Water.

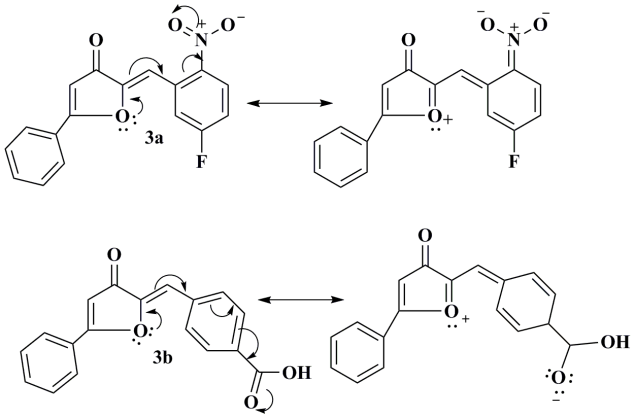

Fig.2. Possible resonance structures of FNPF and CBPF.

When we turn our attention on FNPF alone, it was observed that the shift is moderate on changing the solvent polarity although there is a tendency of shorter absorption maxima even in highly polar acetonitrile.

As stated in the introduction section, the –C=C linkage between the two fragments of both compounds make the charge transfer between the atoms to form fluorescence. In details, as these compounds bear electron donor and acceptor groups, a charge transfer probably occurs in the excited state from the electron–donor to acceptor group by a double bond as a conjugation bridge for charge transfer process. Looking at the molecular structure of these compounds, one can see that the electron donor and acceptor pairs offer resonating structures (Fig. 2), as a result of the ICT. The resonating structures of both compounds are characterized by the participation of electron lone pair on oxygen atom of the furanone to the adjacent carbon. This carbon atom in turn borrows electron density from the neighbouring carbon and so forth and finally increase in charge density on the –NO_2 group in FNPF and in CBPF on the –COOH group. It is imperative to note here that, in this process positive and negative charges are localized in two different and separated functional parts of the molecule resulting in an increase in the molecular dipole moment [27].

The emission spectra (Fig.3 & 4) of both compounds underwent redshift when the polarity of the solvent increased and the effect is more pronounced in CBPF. In case of FNPF, only one emission band was clearly visible at ~430 nm (exceptionally 440 nm in dioxane). But in case of highly polar solvents like water, methanol and acetonitrile, in addition to the short wavelength band a large red-shifted emission band was observed in the wavelength range ~ 454 nm – 461 nm. The short wavelength emission band (~ 427 nm – 430 nm) from a locally excited state appears almost at the same position as the maximum in non-polar solvents. The less fluorescence emitting ability of FNPF in comparison to CBPF can be explained on the basis of strong electron-withdrawing capacity of the nitro group. The nitro group may reduce the fluorescent property by efficient nonradiative decay processes such as singlet-triplet intersystem crossing and internal conversion [28].

Table1. Absorption and emission wavelength maxima (λ_{max}) and photophysical properties of FNPF and CBPF in different homogeneous media.

	λ_{abs}		ε		λ_{emsn}		ϕ_f		τ_f (ns)	
Solvent	FNPF	CBPF	FNPF	CBPF	FNPF	CBPF	FNPF	CBPF	FNPF	CBPF
Water	304	344	1.89	2.12	427(461)	455	0.17	0.004	3.08	1.09
Methanol	309	334	5.80	3.15	430(451)	453	0.19	0.006	3.00	1.09
Acetonitrile	295	329	4.55	3.89	429(454)	484	0.25	0.072	2.57	0.25
Dioxane	316	325	4.78	4.20	440	435	0.47	0.14	2.32	0.14
Tetrahydrofuran	294	326	3.92	4.42	431	424	0.50	0.23	2.60	0.50
Chloroform	316	327	1.20	6.20	432	450	0.56	0.34	2.49	0.56
Cyclohexane	299	326	2.50	1.28	423	417	0.34	0.09	2.21	0.34

In addition to this, the flow of electrons in the acceptor part is hindered owing to the presence of two electron withdrawing groups facing each other.

The fluorescence spectrum of CBPF suffered a strongly bathochromic shift as the solvent polarity increased. This red-shift in the emission maximum from 417 nm in cyclohexane to 484 nm in acetonitrile observably indicates an efficient charge transfer in excited state which is stabilized in polar solvents. On the other hand, in polar protic solvents, a slight blue shift was observed with an increase in solvent polarity for 453 nm in methanol to 455 nm in water.

The blue shift is an indicative of intermolecular hydrogen bond interaction between solvent and solute. Moreover, owing to the planar configuration, both compounds are readily available for hydrogen bonding with protic solvents. All the photophysical parameters relating FNPF and CBPF are listed in Table 1. The absorption and emission spectra of CBPF (Fig.5 & 6) is strongly dependent on the pH. On increasing the pH from 3-11, the absorption spectra were characterized by a peak at the short UV region at 263 nm which was observed to decrease in absorbance with an increase in pH and an isosbestic point at 307 nm was clearly observed. This suggests the presence of two species in this equilibrium but the peak at higher wavelength (345 nm) remains almost unchanged in both absorbance and shift in the wavelength. From figure 6 it is clear that peaks at lower wavelength and higher wavelength show an increase in fluorescence intensity on changing the pH from 3-11. The presence of lone pair of electrons on furanone - oxygen and the electron withdrawing group (–C=O) makes the protonation of CBPF in two ways. In compound CBPF the charge flow from the lone pair of electrons from furanone oxygen to the end carbonyl oxygen favours effective protonation.

However in acidic medium CBPF is stabilized by resonance and additionally the two hydrogen bonding centres (weakly with furanone oxygen and strongly with carbonyl oxygen) ensure an increase in acidic nature for the whole molecule [29]. When the pH is increased from 9 to 11, the fluorescence band is blue-shifted with increase in its intensity. These changes are assigned to the deprotonation of the –COOH group.

The fluorescence lifetimes of CBPF remains almost constant in neat aprotic solvents (range from 2.32 ns to 3.08 ns) whereas shorter lifetimes of 0.72-1.09 ns were observed for FNPF. The lifetimes of both compounds were found to be comparably higher in polar protic solvents. The high quantum yield value signifies the fluorescence nature of this charge transfer compounds. On analysing the presented quantum yield data in Table 1, it is clear that the decrease in solvent polarity strongly enhances the fluorescence quantum yields and this effect is more pronounced in CBPF and this also gives us a hint that there is a strong hydrogen bonding interaction between CBPF and protic solvents [30].

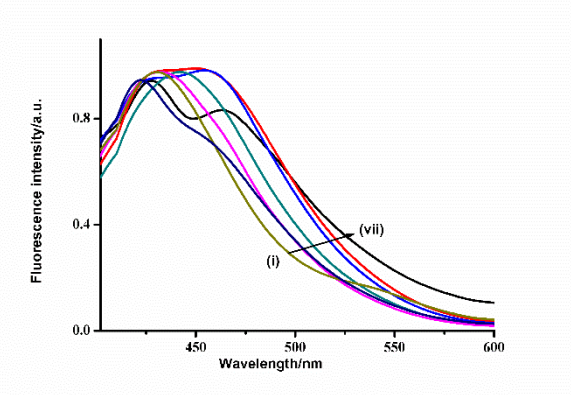

Fig.3. Fluorescence profile of FNPF in different homogeneous solvents: (i) chloroform;(ii) n-cyclohexane; (iii) THF; (iv) dioxane; (v) ACN; (vi) MeoH; (vii) water

On increasing concentrations of water in methanol, the fluorescence intensities of FNPF (Fig.7) decreased dramatically and the fluorescent maxima underwent a slight red shift, due to the increase in the polarity of the solvent. Even more outstanding is the generation of a shoulder peak on increasing the percentage amount of water in solvent mixture. So this observation supports the existence of hydrogen bonded FNPF molecules, as the hydrogen bonded complex absorbs and emits at lower energies. In CBPF, on the other hand (Fig.8) the addition of water in methanol-water mixture remarkably enhances the fluorescence with a slight red shift. This is also

due to the combined effect of hydrogen bonding and polarity of the medium.

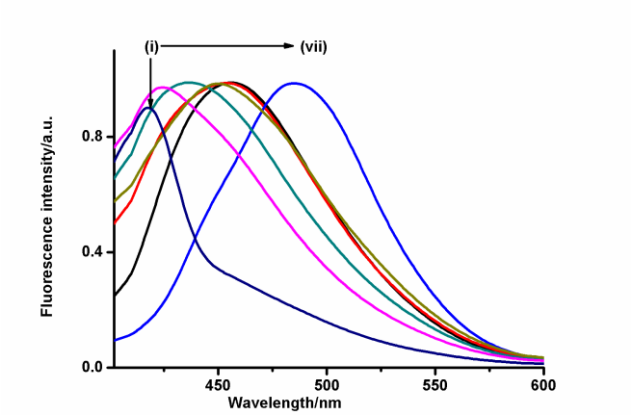

Fig.4. Fluorescence profile of CBPF in different homogeneous solvents: (i) n-cyclohexane (ii) THF (iii) dioxane (iv) chloroform (v) MeoH (vi) water (vii) ACN.

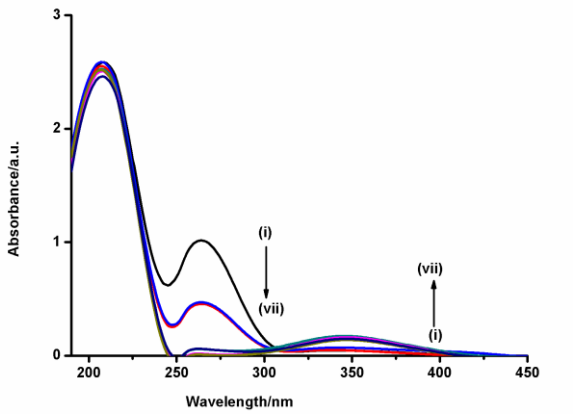

Fig.5.The effect of pH on absorption spectra of CBPF. Curves from top to bottom are pH 3, 4, 5, 7, 9, 10, 11and curves from bottom to top are vice versa.

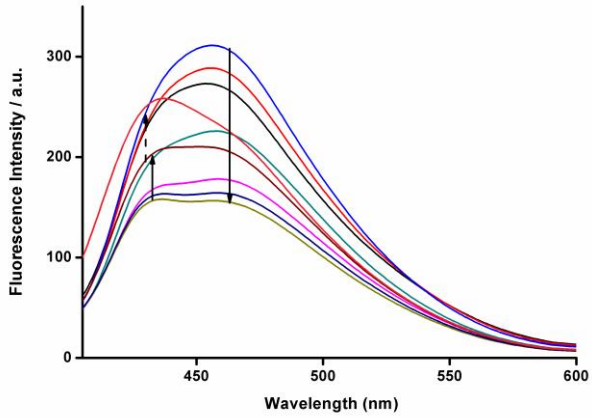

Fig.6. The effect of pH on fluorescence spectra of CBPF. Curves from top to bottom are pH 3, 4, 5, 6, 7, 8; Curves from bottom to top are pH 9, 10, 11.

3.3. Excited state dipole moments calculation

The dipole moment of a molecule in the excited-state is determined by the effect of electric field (internal or external) on the position of its spectral band. The solvent dependence of the absorption and fluorescence maxima is used to estimate the excitation-state dipole moments of different molecules. Equations (1) and (2) that afford the best results in the change of dipole moments of an excited molecule were suggested by Kawski and Bojarski Bakhshiev's equation [31].

$$\bar{\upsilon}_a - \bar{\upsilon}_f = S_1F_1(\varepsilon, n) + \text{Const} \quad (1)$$

Kawski-Chamma-Viallet' equation [32]

$$\frac{\bar{\upsilon}_a + \bar{\upsilon}_f}{2} = S_2F_2(\varepsilon, n) + \text{Const} \quad (2)$$

Where, $F_1(\varepsilon, n)$ [Bakhshiev's polarity function] and $F_2(\varepsilon, n)$ [Kawski-Chamma-Viallet's polarity function] are given below

$$F_1(\varepsilon, n) = \frac{2n^2+1}{n^2+2}\left[\frac{\varepsilon-1}{\varepsilon-2} - \frac{n^2-1}{n^2+2}\right] \quad (3)$$

$$F_2(\varepsilon, n) = \frac{2n^2+1}{2(n^2+2)}\left[\left(\frac{\varepsilon-1}{\varepsilon-2} - \frac{n^2-1}{n^2+2}\right) + \frac{3(n^4-1)}{2(n^2+2)^2}\right] \quad (4)$$

Where $\bar{\upsilon}_a$ and $\bar{\upsilon}_f$ are the absorption and fluorescence maxima wave numbers in cm^{-1}, respectively, n and ε are the refractive index and the dielectric constant of the solvents. From Eqns. (1) - (4), it follows that $(\bar{\upsilon}_a - \bar{\upsilon}_f)$ versus $F_1(\varepsilon, n)$ and $\frac{\bar{\upsilon}_a + \bar{\upsilon}_f}{2}$ versus $F_2(\varepsilon, n)$, plots represent linear graphs with slopes S_1 and S_2 respectively. Using these slopes the ground state dipole moment, μ_g and the excited state dipole moment, μ_e can be obtained [33].

By examining the solvent effect on FNPF and CBPF, it is clear that the shifts of emission peaks with solvent polarity changes are predominant than the shifts of absorption peaks. This indicates that $\Delta\mu$ is positive i.e. the dipole moment of both molecules increases on excitation.

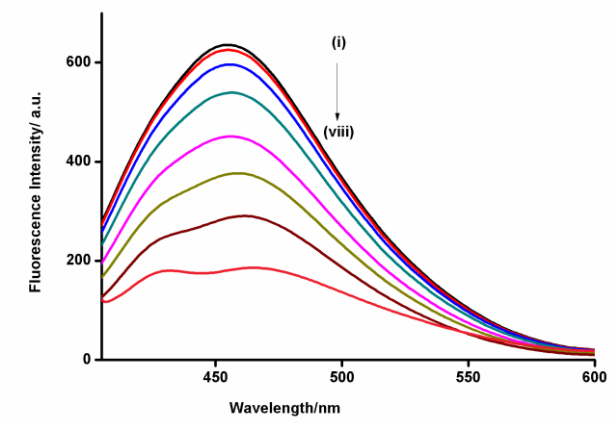

Fig.7. Emission spectra of FNPF in methanol as a function of water percentage composition; represents the curves (i) to (viii) correspond to 0%, 5%, 10%, 20%, 40%, 60%, 90%, 100% water (v/v), respectively.

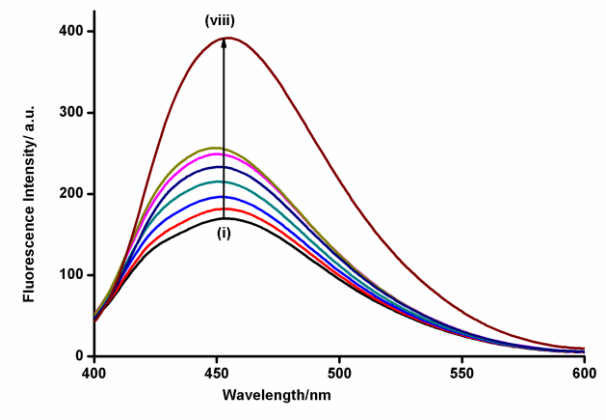

Fig.8. Emission spectra of CBPF in methanol as a function of water percentage composition; represents the curves (i) to (viii) correspond to 0%, 5%, 10%, 20%, 40%, 60%, 90%, 100% water (v/v), respectively.

Table S1 summarises the Stokes shift data for FNPF and CBPF along with the solvent polarity function values F1 (ε, n) and F2 (ε, n) of various solvents. Fig. 9 & 10 shows the graphs of spectral shifts ($\bar{\upsilon}_a$-$\bar{\upsilon}_f$) versus bulk solvent polarity functions F1 (ε, n) and Fig. 11 & 12 shows the graph of respective spectral shifts versus bulk solvent polarity functions F2 (ε, n), from which the slopes S1 and S2 were obtained. The linear behaviour of Stokes shift with solvent polarity functions indicates general solvent effects as a function of dielectric constant and refractive index.

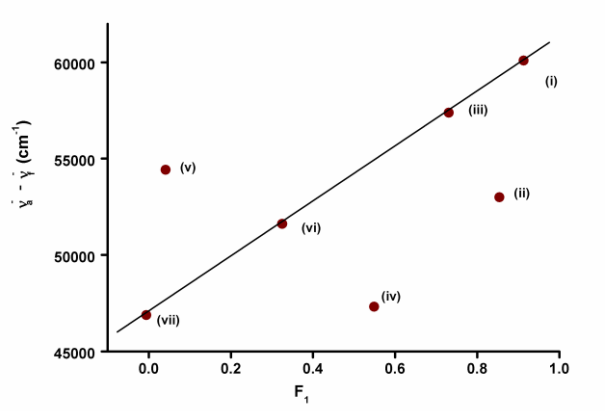

Fig.9. The variation of Stokes shift of FNPF with F_1 (ε, n) by using Bakhshiev's equation. The numbers refer to the solvents: (i) water; (ii) MeoH; (iii) ACN; (iv) THF; (v) dioxane; (vi) chloroform; (vii) n-cyclohexane.

The estimated dipole moment differences were 3.47 D (Debye) for FNPF and 3.3 D of CBPF based on the assumption that the Onsager cavity radius 'a' equals to 4.72 Å and 5.2 Å respectively, which were 40% of the optimized distance between the two farthest atoms of the molecule in the direction of charge separation [34]. This large change in dipole moment from ground to excited state can also be explained in terms of their possible resonance structure as shown in Fig 2.

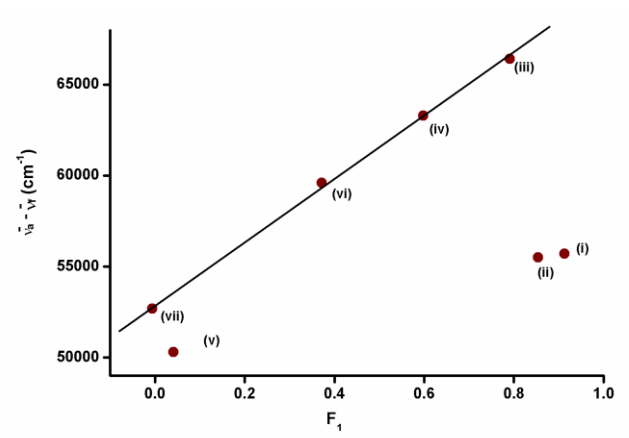

Fig.10. The variation of Stokes shift of CBPF with F_1 (ε, n) by using Bakhshiev's equation. The numbers refer to the solvents: (i) water; (ii) MeoH; (iii) ACN; (iv) THF; (v) dioxane; (vi) chloroform; (vii) n-cyclohexane

The contributing resonance structures stem out of the delocalization of π- electrons from the π- excessive furanone ring to the phenyl ring attached with the substituents. This charge transfer accompanying excitation to lowest excited singlet-state, usually results in the excited molecule having larger dipole moment than the ground state molecule.

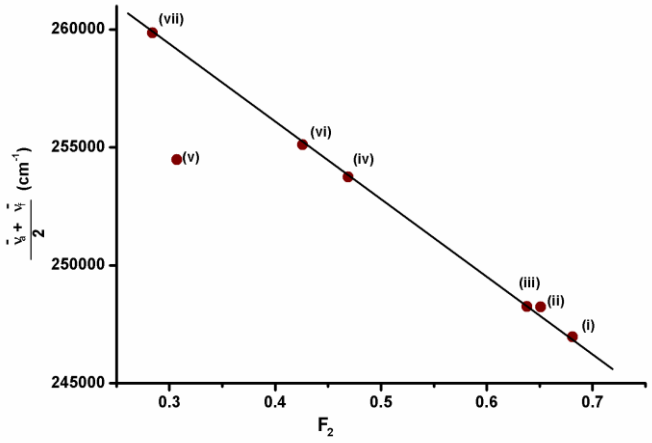

Fig.11. The variation of Stokes shift of FNPF with F_2 (ε, n) by using Kawski-Chamma-Viallet's equation. The numbers refer to the solvents: (i) water; (ii) MeoH; (iii) ACN; (iv) THF; (v) dioxane; (vi) chloroform; (vii) n-cyclohexane.

3.4. Voltammetric behaviour of CBPF and FNPF

The cyclic voltammetric behaviour of both compounds (CBPF and FNPF) (Fig. 13) shows an irreversible reductive peaks at -1068 mV and -1114 mV respectively, confirming the reduction of –C=C– bridge between the furanone and phenyl moiety.

In addition, FNPF also gives a sharp cathodic peak at -866 mV and a corresponding anodic peak at -760 mV, showing an apparently quasireversible behaviour of the electrode reaction [35]. This quasireversible peak is due to the reversible mono-electron reduction of nitro group to the radical anion.

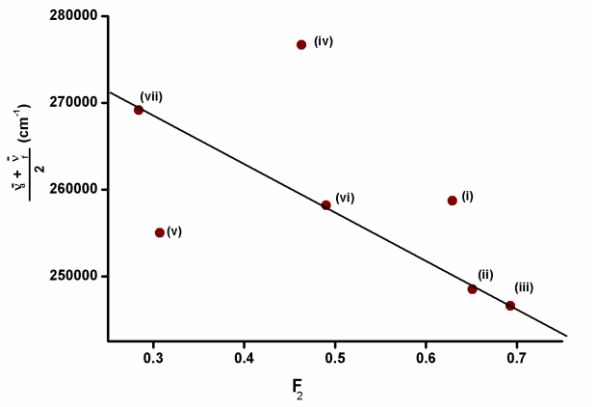

Fig.12. The variation of Stokes shift of CBPF with F_2 (ε, n) by using Kawski-Chamma-Viallet's equation. The numbers refer to the solvents: (i) water; (ii) MeoH; (iii) ACN; (iv) THF; (v) dioxane; (vi) chloroform; (vii) n-cyclohexane.

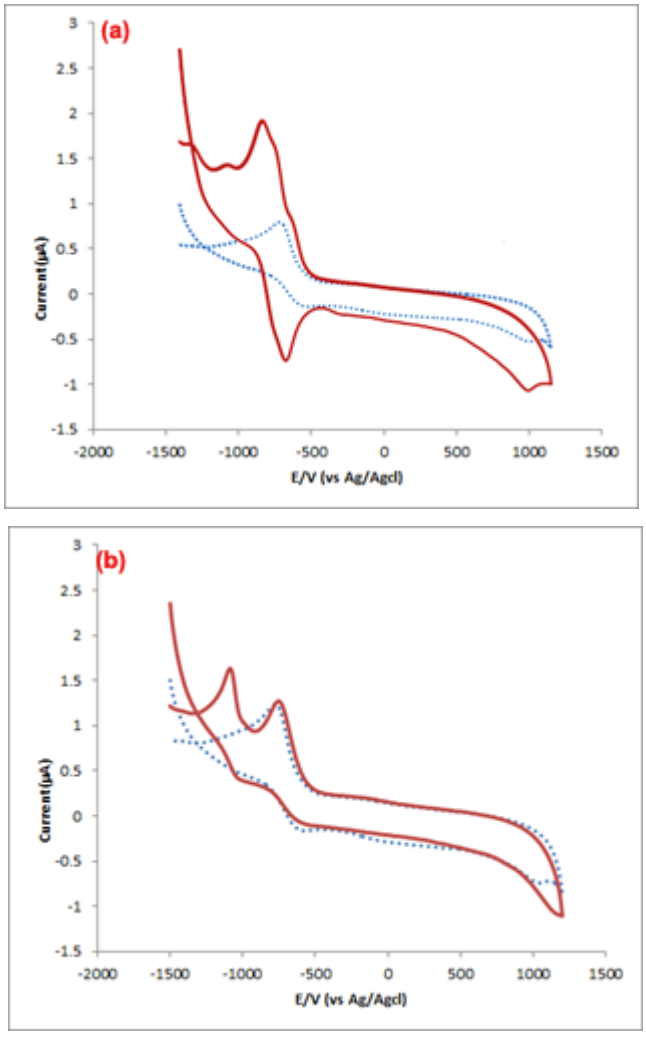

Fig.13. Cyclic voltammograms of 1×10^{-3} M of (a) FNPF (b) CBPF in DMSO with 0.1M Lithium perchlorate ($LiClO_4$) *vs* Ag/AgCl and GC electrodes at a sweep rate of 50 mV/sec. The dashed line shows the corresponding blank solution.

3.5. Quantum chemical calculation

Using quantum chemical calculations, both compounds FNPF and CBPF were optimized in ground and excited states. Additionally, TD-DFT calculations of the excited and ground states were performed.

The optimized geometrical structures of title compounds are shown in Fig. 14. Selected geometrical parameters, such as bond length, and dihedral angles are compiled in Table 2. The bond length of the –C=C– bond bridging the furanone and the substituted phenyl groups is calculated to be 1.380 Å and 1.353 Å for FNPF and CBPF respectively in its excited state. A significant decrease in the bond length of –C4–O5 (1.39 Å) for both compounds than normal C–O bond length (1.43 Å) suggests that electron lone pair on the furanone O5 atom can be easily delocalized towards the electron deficient end fragment. The important dihedral angles which supply valuable information about the planarity of FNPF are O5-C4-C12-H30 (D_1), O5-C4-C12-C13 (D_2), C16-C15-N20-O23 (D_3) and of CBPF are O5-C4-C12-H29 (D_1), O5-C4-C12-C13 (D_2) and C16-C17-C20-O2 (D_3). From the data presented in Table 2 it is clear that all these atoms are adopting the perfect angle of 180^0 or 0^0 wherever required to give structural planarity. This ascertain our assumption that the furanone and the substituted phenyl ring adopt a nearly coplanar orientation with the –C=C–. Such an orientation is expected to allow for efficient electronic interaction between these groups.

The HOMO and LUMO diagrams of FNPF and CBPF are shown in Figure S15. The effect of solvent polarity on the frontier orbitals and their corresponding energy gaps were examined. It is apparent from these figures that the electron density distribution of the HOMOs and LUMOs of FNPF and CBPF in gas phase and cyclohexane are comparable. For FNPF the electron density distribution of HOMO is fully localized on 5-phenyl furan 3-(2H) one with a minor contribution on substituted phenyl ring. It was observed that the electron density was fully populated on the furanone ring in polar solvent water and this effect is likely due to the stabilization of the HOMO orbital. Interestingly, LUMO electron density of FNPF shows that the electron cloud shifts more toward the substituted phenyl ring on the right owing to the presence of strong electron- withdrawing nitro group. This indicates that the electron flow is from the 5-phenyl furan-3-(2H)one to the substituted phenyl ring, which belongs to π-π^* transition. As expected the HOMOs and LUMOs of CBPF are better distributed over the whole molecular skeleton in all media confirming its extensive delocalization of π-electrons throughout the system. Therefore, the electronic transitions for both compounds from HOMO to LUMO could lead to an intramolecular charge transfer from the donor to the anchoring groups through the conjugated bridge, so that the HOMO-LUMO transition can be classified as π-π^*.

The calculation results for the first singlet excitation energies and oscillator strengths are summarized in Table 3. Experimental results show a bathochromic shift of emission maxima when the solvent is changed from cyclohexane to

water and this shift is correctly reproduced by the calculations for both compounds. The dipole moments of the compounds were computed in gas phase and also in highly polar and non-polar solvents by TD-DFT to investigate the electronic behaviour from ground state to excited state. The trends in the dipole moment values reveal that the structures in the excited state exhibited higher diploe moments in comparison to the ground state. These observations are in line with the experimental results, as these compounds demonstrated positive solvatochromic effect when the polarity of the solvent was increased.

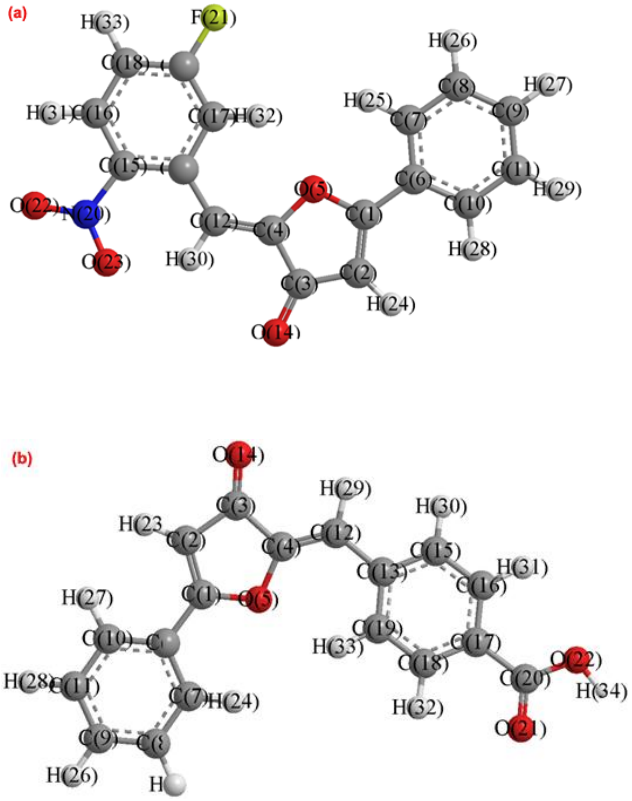

Fig.14. The optimized geometrical structures of (a) FNPF and (b) CBPF calculated at B3LYP/6-31G+ (d, p) level with GaussView 05.

***Table 2**. Theoretically calculated geometrical parameters (B3LYP-6-31+G(d, p)) of FNPF and CBPF in the excited state*

Bondlength A^0 / Dihedral angle^0	*FNPF*	*CBPF*
D_1	*180*	*178.44*
D_2	*0*	*-0.629*
D_3	*179.99*	*179.92*
C4-C12	*1.38*	*1.35*
O5-C4	*1.39*	*1.39*
C12-C13	*1.43*	*1.47*
C13-C15	*1.44*	*1.40*
C15-N20	*1.45*	*-*
N20-O23	*1.24*	*-*
N20-O22	*1.24*	*-*
C15-C16	*-*	*1.39*
C16-C17	*-*	*1.40*
C17-C20	*-*	*1.48*
C20-O22	*-*	*1.34*
C20-O21	*-*	*1.22*

D_1 - O5-C4-C12-H30/ O5-C4-C12-H29, D_2- O5-C4-C12-C13/ O5-C4-C12-C13, D_3- C16-C15-N20-O23/ C16-C17-C20-O2

4. Conclusions

A new class of fluorescent dyes based on 2(3H)-furanone has been designed and characterized. The synthetic strategy is straight forward and on replacing the acceptor unit with an even larger flat aromatic systems might further advance its properties. The solvent effect on the fluorescence characteristics of (2Z)-2-(5-fluoro-2-ntro benzylidene)-5-phenyl-3(2H)-furanone (FNPF) and (2Z)-2-(4-carboxy benzylidene)-5-phenyl-3-(2H)-furanone (CBPF) indicated that the emission wavelengths of these compounds are red-shifted with the increase of solvent polarity. Hence it can be concluded that there is an ample scope for further study in developing these as good lead compounds which may be useful for bio analytical purposes and are addition in the library of new heterocyclic compounds.

Table 3. HOMO–LUMO energies (eV), HOMO–LUMO energy gap (eV), absorption and emission wavelengths (nm), oscillator strengths (f) and dipole moments (Debye) calculated at (B3LYP-6-31+G(d, p)) level for FNPF and CBPF

Parameter	FNPF						CBPF					
	Ground state			Excited state			Ground state			Excited state		
	GP	water	Chx	GP	water	Chx	GP	water	Chx	GP	water	Chx
E_{HOMO}(eV)	-0.293	-0.293	-0.297	-0.264	-0.278	-0.284	-0.247	-0.295	-0.290	-0.245	-0.277	-0.246
E_{LUMO}(eV)	-0.123	-0.140	-0.138	-0.104	-0.106	-0.104	-0.113	-0.142	-0.124	-0.112	-0.125	-0.112
E_g(eV)	0.170	0.153	0.159	0.16	0.172	0.18	0.134	0.153	0.166	0.133	0.152	0.134
λ_1 (nm)/f	305.5/ 0.44	320.4/ 0.72	291.0/ 0.67	431.2/ 0.86	469.0/ 0.67	425.8/ 0.67	330.5/ 0.66	364.0/ 1.04	340.7/ 0.85	422.8/ 0.60	446.4/ 0.62	420.2/ 0.70
μ (D)	7.8	10.4	10.1	8.8	12.3	11.2	3.03	2.4	2.1	3.9	3.9	3.4

GP, gas phase; Chx, cyclohexane.

Acknowledgements

Beena Varghese would like to thank SQU for the PhD scholarship.

References

1 KT. Plajnsek, S. Pajk, B. Govedarica, S. Pecar, S. Srcic, J. Kristl, *International Journal of Pharmaceuticals*, 2011, **416**, 384-393.
2 EM. Flefel, RE. Abdel-Mageid, WA. Tantawy, MA. Ali, AE-GE. Amr, *Acta Pharmaceutica*, 2012, **62**, 593-606.
3 SN. Murty, B. Madhav, AV. Kumar, KR. Rao, YVD. Nageswar, *Tetrahedron*, 2009, **65**, 5251-5256.
4 WS. Sung, HJ. Jung, K. Park, HS. Kim, I-S. Lee, DG. Lee, *Life Sciences*, 2007, **80**, 586-591.
5 AH. Banskota, JB. McAlpine, D. Sorensen, M. Aouidate, M. Piraee, A-M. Alarco, S. Omura, K. Shiomi, EZ. Farnet, *The journal of Antibiotics*, 2006, **59**, 168-176.
6 CM. Marson, E. Edaan, JM. Morrell, SJ. Coles, MB. Hursthouse, DT. Davies, *Chemical Communications*, 2007, 2494-2496.
7 E. Lattmann, WO. Ayuko, D. Kinchinaton, CA. Langley, H. Singh, L. Karimi, MJ. Tisdale, *Journal of Pharmacy and Pharmacology*, 2003, **55**, 1259-1265.
8 Y. Chen, M. Cheng, F. Liu, P. Xia, K. Qian, D. Yu, Y. Xia, Z-Y. Yang, C-H. Chen, SL. Morris-Natschke, K-H. Lee, *European Journal of Medicinal Chemistry*, 2009, **46**, 4924-4936.
9 V. Nardini, SMM. Rodrigues, GVJS. Constantino, *Molecules*, 2012, **17**, 12151-12162.
10 B. Crone, SF. Kirsch, *The Journal of Organic Chemistry*, 2007, **72**, 5435-5438.
11 PG. Baraldi, S. Manfredini, D. Simoni, MA. Tabrizi, J. Balzarini, ED. Clercq, *Journal of Medicinal Chemistry*, 1992, **35**, 1877-1882.
12 P. Langer, T. Krummel, *Chemical Communications*, 2000, 967-968.
13 PK, Gupta, JG. Jones, E. Caspi, *The Journal of Organic Chemistry*, 1975, **40**, 1420.
14 V. Georgiev, RA. Mack, CR. Kinsloving, *Heterocycles*, 1986, **24**, 3195.
15 C. Stefano, B. Marco, C. Barbara, D. Franscesco, V. Giampietro, *Tetrahedron*, 2003, **59**, 5215-5223.
16 Y. Liu, M. Liu, S. Guo, H. Tu, Y. Zhou, H. Gao, *Organic Letters*, 2006, **8**, 3445.
17 S. Al-Busafi, M. Al-Belushi, K. Al-Muqbali, *Synthetic Communications*, 2010, **40**, 1088-1092.
18 C. Qi, H. Jiang, L. Huang, G. Yuan, Y. Ren, *Organic Letters*, 2011, **13**, 5520.
19 T. Kusakabe, T. Takahashi, R. Shen, A. Ikeda, YD. Dhage, Y. Kanno, Y. Inouye, H. Sasai, T. Mochida, K. Kato, *Angewandte Chemie International Edition*, 2013, **52**, 7845.
20 D. Yin, W. Wang, Y. Peng, Z. Ge, T. Cheng, X. Wang, R. Li, *RSC Advances*, 2015, **5** , 17296.
21 H. He, C. Qi, X. Hu, L. Ouyang, W. Xiong, H. Jiang, *Journal of Organic Chemistry*, 2015, **80**, 4957.
22 G. Chen, H-Y. Wang, Y. Liu, X-P. Xu, S-J. Ji, *Dyes and Pigments*, 2010, **85**, 194.
23 AD. Becke, *Physical Review A*, 1988, **38**, 3098.
24 C. Lee, W. Yang, RG. Parr, *Physical Review B: Condensed Matter and Materials Physics*, 1988, **37**, 785-789.
25 JB. Foresman, M. Head-Gordon, JA. Pople, MJ. Frisch, *Journal of Physical Chemistry*, 1992, **96**, 135.
26 S. Miertus, E. Scrocco, J. Tomasi, *Chemical Physics*, 1981, **55**, 117.
27 SK. Saha, P. Purkayastha, AB. Das, *Journal of photochemistry and photobiology A: Chemistry*, 2008, **195**, 368.
28 MK. Saroj, N. Sharma, RC. Rastogi, *Journal of Fluorescence*, 2011, **21**, 2213.
29 J. Qian, Y. Xu, X. Qian, S. Zhang, *Journal of photochemistry and photobiology A: Chemistry*, 2009, **207**, 181.
30 SA. El-Daly, AM. Asiri, SA. Khan, KA. Alamry, *Journal of Luminescence*, 2013, **134**, 819.
31 JS. Kadadevarmath, GH. Malimath, NR. Patil, HS. Geethanjali, RM. Melavanki, *Canadian Journal of Physics*, 2013, **91**, 1107.
32 MM. Husain, R. Sindhu, HC. Tandone, *European Journal of Chemistry*, 2012, **3**, 75.
33 VD. Gupta, VS. Padalkar, KR. Phatangare, VS. Patil, PG. Umape, N. Sekar, *Dyes and Pigments*, 2011, **88**,307.
34 S. Song, D. Ju, J. Li, D. Li, Y. Wei , C. Dong, P. Lin, S. Shuang, *Talanta*, 2009, **77**, 1707.
35 RJ. Mascarenhas, I. Namboothiri, BS. Sherigara, VK. Reddy, *Journal of Chemical Sciences*, 2006, **118**, 275.